European Journal of Medicinal Chemistry 79 (2014) 95–101

Contents lists available at ScienceDirect

European Journal of Medicinal Chemistry

journal homepage: http://www.elsevier.com/locate/ejmech

Original article

Synthesis of 6-cinnamoyl-2*H*-benzo[b][1,4]oxazin-3(4*H*)-ones and their effects on A549 lung cancer cell growth

Xue-Wen Zhou [a,1], Han-Lin Ma [b,1], Xuan Zhang [a], Shi-Yao Jing [a], Jun-Ying Miao [b,*], Bao-Xiang Zhao [a,*]

[a] Institute of Organic Chemistry, School of Chemistry and Chemical Engineering, Shandong University, Jinan 250100, PR China
[b] Institute of Developmental Biology, School of Life Science, Shandong University, Jinan 250100, PR China

ARTICLE INFO

Article history:
Received 16 January 2014
Received in revised form
28 March 2014
Accepted 31 March 2014
Available online 1 April 2014

Keywords:
Benzoxazinone
Chalcone
A549 lung cells
Autophagy

ABSTRACT

A series of novel 6-cinnamoyl-2*H*-benzo[b][1,4]oxazin-3(4*H*)-one derivatives was synthesized. The structures of compounds were characterized by ^{1}H NMR, IR, and MS. Moreover, representative crystal structure was determined by X-ray diffraction analysis. The preliminary biological evaluation of all these compounds showed that compounds **3a**–**3d** would suppress the growth of A549 lung cells effectively by inducing autophagy and cell cycle arrest.

1. Introduction

With the increasingly serious environmental problems and the dramatic increase of smoking rate, lung cancer is becoming primary cause of cancer-related mortality not only in China but also around the world. It has been believed that the primary modality for the treatment of lung cancer is chemotherapy. Consequently, much attention has recently been paid to the discovery and development of new, more selective anticancer agents [1–4].

The common method of lung cancer chemotherapy issue effective drugs for the treatment of patient [5]. Different mechanisms of drug-induced death of cancer cells are not the same. Therefore, the understanding of mechanisms of cancer cells death can help us discover more convenient therapeutic strategies [6]. Several mechanisms of cell death including necrosis, apoptosis and autophagy have been known [7]. However, we cannot expect the mechanism by which a new small molecule inhibits cancer cell growth. Therefore, it needs to design and synthesize new compounds and screen effective lung cancer cell growth inhibitor.

Compounds of benzoxazinone class, with the modifiable skeleton and relative accessibility, have attracted much attention of chemists [8–11]. Benzoxazinone derivatives have a broad range of biological activities, such as treatment of cardiovascular diseases [12–14], antibacterial [15,16], antifungal [17–19], anticancer activity [20–22] and protein methyltransferases inhibitors [23].

Chalcones consist of two aryl rings linked by α,β-unsaturated carbonyl system, which are members of flavonoids. Chalcone derivatives have occupied an important position in drug discovery, such as anti-inflammatory [24,25], antimicrobial activity [26–29], anti-parasitic activity [30,31], acetylcholine esterase inhibition [32], antidyslipidemic [33] and anticancer activity [34–38].

Based on the advantages of benzoxazinone and chalcone moieties, we are interested in combining these active moieties to design and synthesize new compounds and test their biological activity. Herein we would like to report the synthesis, crystal structure of 6-cinnamoyl-2*H*-benzo[b][1,4]oxazin-3(4*H*)-ones and the findings of their biological activities against A549 lung cancer cell growth and possible function mechanisms.

2. Chemistry

2.1. Synthesis

We designed and synthesized compounds **3a**–**3g** as shown in Scheme 1. Compound **2** was obtained by Friedel–Crafts acylation,

* Corresponding authors.
E-mail addresses: miaojy@sdu.edu.cn (J.-Y. Miao), bxzhao@sdu.edu.cn, sduzhao@hotmail.com (B.-X. Zhao).
[1] Equal contribution.

http://dx.doi.org/10.1016/j.ejmech.2014.03.087
0223-5234/

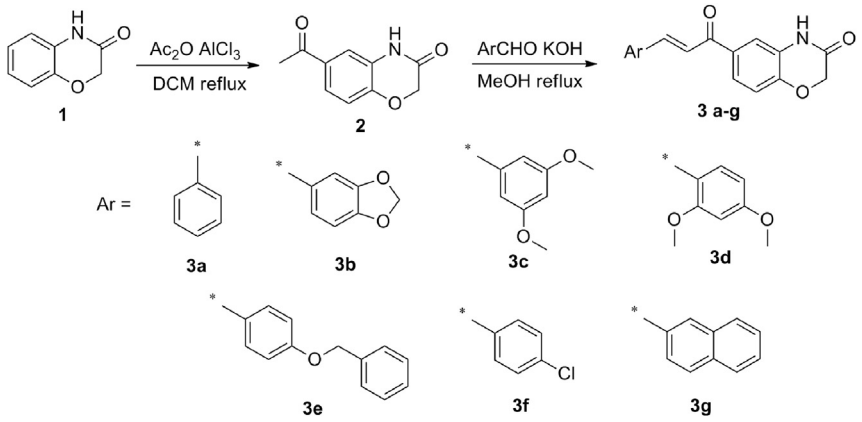

Scheme 1. Synthesis of 6-cinnamoyl-2*H*-benzo[b][1,4]oxazin-3(4*H*)-ones.

and then, reacted with corresponding aldehyde to get the target products.

2.2. Single-crystal structural characterization by X-ray

The spatial structure of compound **3a** was determined by X-ray diffraction analysis. The single crystal was grown from ethyl acetate solution at room temperature. The molecular view of **3a** is shown in Fig. 1. The molecule of **3a** consists three fragments, an aryl ring, a benzoxazinone, and α,β-unsaturated carbonyl system.

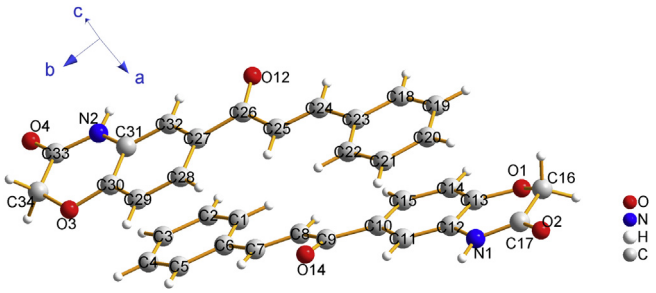

Fig. 1. The X-ray crystal structure of compound **3a**.

3. Pharmacology

Screening of synthesized substances was carried out using lung cancer A549 cell line. Proliferation percentage was determined by the SRB assay. Cells were incubated with compounds at 1, 5 and 10 μM for 48 h and the cell proliferation/viability determination using the survival percentage obtained with the cell treated only with the solvent (DMSO at 0.1%) as reference. The results are expressed as the average of triplicate assays.

4. Results and discussion

4.1. Compounds *3a*–*3g* inhibited proliferation of A549 lung cancer cells

In order to examine the anti-cancer activity of compounds **3a**–**3g**, we firstly observed the morphological changes of A549 cells after treatment with the compounds for 24 h or 48 h with a phase contrast microscope (Fig. 2). We found no obvious morphological changes in A549 cells treated with 5 μM dose of each compound for 48 h. However, the cell density greatly decreased in response to compounds **3a**–**3d** compared with control group. SRB assay showed that compounds **3a**–**3d** inhibited the growth of A549 cells in dose dependent manner after treatment with the compounds for 48 h (Fig. 3). Among the four compounds, compound **3c** (10 μM) showed the most obvious effect and could inhibit the viability of A549 cells to 24% compared with control group. Table 1 showed compounds **3a**, **3c** and **3d** have lower IC_{50} value.

4.2. Compounds *3a*–*3d* showed different effect on autophagy of A549 cells

Autophagy is a basic homeostatic process working in almost every mammalian cell types and plays a key role in cell survival mechanism [39]. Paradoxically, autophagy plays an important role both in protective process and cell death [40]. Therefore, it is very complex between autophagy and cancer treatment due to the pro-survival and pro-death functions of autophagy. In the early stage of cancer progression, enhanced autophagy has been regarded as the inhibitor of tumor genesis through degradation of oncogenic proteins. On the other hand, in the late stages of oncogenesis, autophagy may assist tumor cells against metabolic stress and resist death caused by chemotherapeutic [40–42].

In order to determine the changes of autophagy in the growth inhibitory effect of compounds **3a**–**3d**, firstly, we performed acridine orange (AO) staining. After treatment with compounds **3a**–**3d** (5 μM) for 48 h (Fig. 4), compounds **3c**, **3d** could apparently increase the acidic vesicles accumulation in A549 cells compared with control, however, there was no clear facilitation effect in compounds **3a**, **3b** treated groups. These results suggested that compounds **3a**–**3d** may have different effect on autophagy of A549 cells.

To exhibit a far more explicit function of compounds **3a**–**3d** on autophagy of A549 cells, we detected the protein level of LC3-II (Fig. 5), the up regulation of which means the promotion of autophagy [43]. Western blotting assay showed that the expression of LC3-II promoted after treatment with compounds **3c**, **3d** (5 μM) for 48 h, whereas compound **3b** had no effect on LC3-II protein level. Interestingly, in contrast with compounds **3c, 3d**, compound **3a** could inhibit the expression of LC3-II protein. The study of structure–activity relationship showed that compounds with multiple methoxy groups and no substituent group in aryl moiety altered the antitumor effect significantly. The underlying mechanism by which compounds **3a**–**3d** function on the autophagy of A549 cells needed to be further investigation.

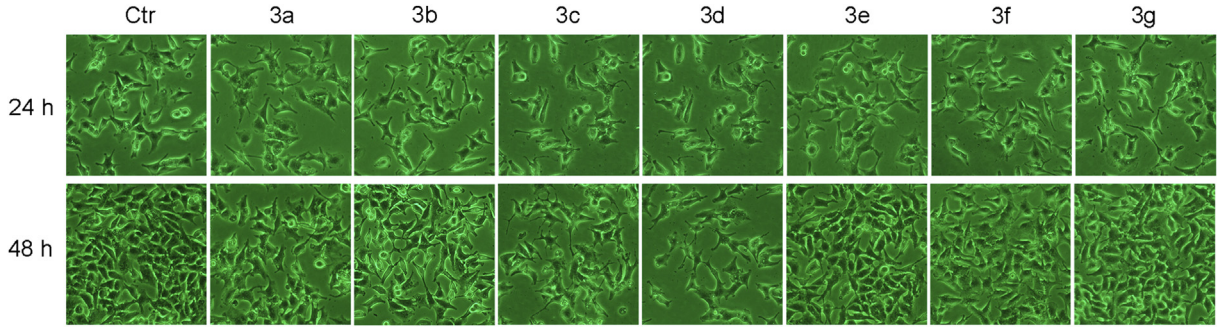

Fig. 2. Effects of the compounds **3a**–**3g** on morphology of A549 cells. A549 cells were treated with **3a**–**3g** (5 μM) or 0.1% DMSO (control) for 24 h or 48 h.

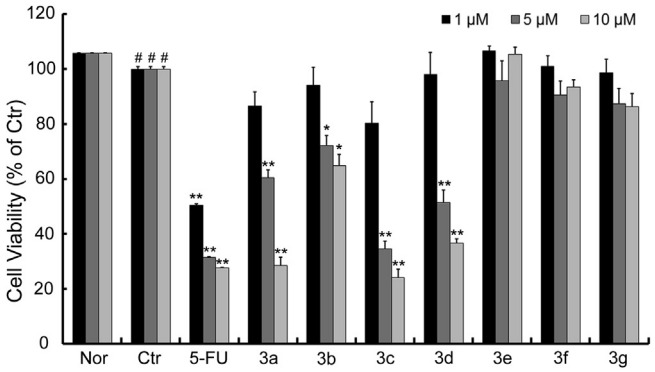

Fig. 3. Effects of compounds **3a**–**3g** on A549 cell viability. Cells were treated with compounds **3a**–**3g**, 5-FU and 0.1% DMSO (control) at the concentration of 1, 5 or 10 μM for 48 h. Cell viability was analyzed by SRB assay. Results were presented as mean ± SE ($n = 3$, $^{*}p < 0.05$ vs. control; $^{**}p < 0.01$ vs. control; ##p<0.01vs. normal).

4.3. Compounds *3a*–*3d* induced G_1-phase arrest

One main feature of cancer cells is multiply uncontrollably. In tumors, there are much more cells that are in active cell division compared with the normal tissues [44]. So, cell cycle arrest becomes a critical therapy target in oncotherapy [45,46]. Flow cytometric analysis indicated that compounds **3a**–**3d** (5 μM) could induce A549 cell cycle arrest in G1-phase after treatment for 48 h. Compound **3c** showed the best effect and could enhance the G1 population by 24.76% compared with control group. Meanwhile, the portion of cells in G2-phase had a slight increase after treatment with compounds **3a**–**3d** (5 μM) for 48 h (Fig. 6).

4.4. Compounds *3a*–*3d* did not induce apoptosis in A549 cells

Apoptosis, the process of programmed cell death (PCD), is an important therapy target for cancer chemotherapy. Biochemical events cause characteristic cell changes, including nuclear fragmentation, chromatin condensation and the fragmentation of chromosomal DNA [47,48]. Hoechst 33258 staining was performed to detect the effect of compounds **3a**–**3d** on apoptosis of A549 cells (Fig. 7). After treatment with compounds **3a**–**3d** (5 μM) for 48 h, there were no obvious chromatin condensation and increase in the formation of apoptotic bodies compared with control group. Thus, the compounds **3a**–**3d** (5 μM) did not induce apoptosis in A549 cells at 48 h significantly.

Table 1
IC_{50} of the compounds **3a**–**3d** and 5-FU for A549 cells at 48 h.

Compounds	5-FU	3a	3b	3c	3d
IC_{50} (μM)	0.98	5.46	16.31	3.29	6.49

4.5. Compounds *3a*–*3d* did not cause necrosis in A549 cells

To determine whether the proliferation inhibitory effects of compounds **3a**–**3d** were due to necrosis or not, which is undesired in cancer therapy, we detected the LDH level after treatment with compounds **3a**–**3d** (10 μM) for 48 h, the up regulation of which is an indicator of necrosis. Results showed that compounds **3a**–**3d** (10 μM) did not cause necrosis in a certain period of time (48 h) in A549 cells (Fig. 8).

5. Conclusion

In summary, we have synthesized a series of novel 6-cinnamoyl-2*H*-benzo[b][1,4]oxazin-3(4*H*)-ones by the condensation of 6-acetyl-2*H*-benzo[b][1,4]oxazin-3(4*H*)-one and corresponding aromatic aldehydes. Compounds **3a**–**3d** can suppress the growth of A549 lung cancer cells by inducing autophagy and cell cycle arrest.

6. Experimental

6.1. Reagents and apparatus

All reagents were of analytical grade or chemically pure. Analytical TLC was performed on silica gel 60 F_{254} plates (Merck KGaA). Melting points were determined on an XD-4 digital micro-melting point apparatus. HRMS spectra were recorded on a LTQ Orbitrap Hybrid mass spectrograph. ^{1}H NMR spectra were recorded on a Bruker Avance 400 (400 MHz) spectrometer or Bruker Avance 300 (300 MHz) spectrometer, using DMSO as solvent and tetramethylsilane (TMS) as an internal standard.

6.2. Preparation of 6-acetyl-2H-benzo[b][1,4]oxazin-3(4H)-ones (*2*)

Compound **1** (20 mmol), aluminum chloride (100 mmol) and 100 ml dry CH_2Cl_2 were added in round-bottom flask equipped with calcium chloride guard tube under ice bath for 30 min, then Ac_2O (20 mmol) was added to the mixture. The reaction mixture was refluxed for 5 h, monitored by TLC until completion. The mixture was diluted with water and filtered. The filtrate was washed with saturate $NaHCO_3$ solution (100 ml × 2), and water (100 ml × 1), dried over anhydrous Na_2SO_4, and filtered. The filtrate was concentrated under reduced pressure. Recrystallization from ethanol afforded the pure products **2**.

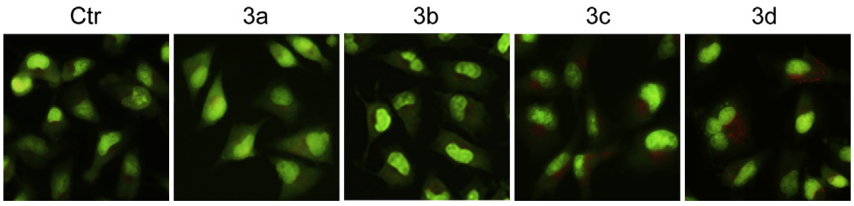

Fig. 4. Effects of compounds **3a**–**3d** (5 μM) on acidic vesicles accumulation in A549 cells after treatment for 48 h. Microscopic photographs (200×) were taken under a fluorescent microscope (Nikon).

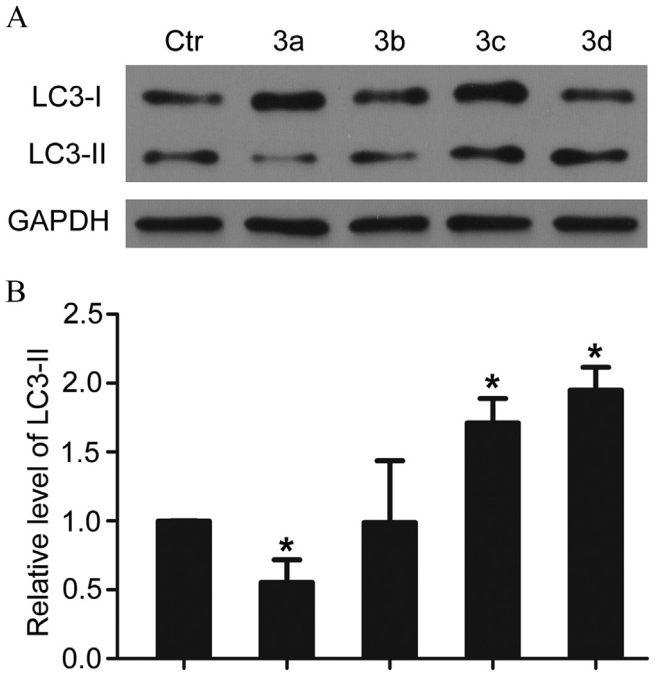

Fig. 5. Effects of compounds **3a**–**3d** (5 μM) on the protein level of LC3-II. Cells were treated with compounds **3a**–**3d** (5 μM) for 48 h. The protein levels of LC3-II were determined by Western blotting (A). The relative levels of LC3-II were normalized to the level of GAPDH and represented as percent of control (B) ($n = 3$, $^*P < 0.05$ vs. control).

6.3. Preparation of 6-cinnamoyl-2H-benzo[b][1,4]oxazin-3(4H)-ones (**3a**–**3g**)

Compound **2** (1.5 mmol), corresponding aldehyde (1.8 mmol), sodium hydroxide (3 mmol) and 40 ml methanol were added into round-bottom flask, then the reaction mixture was refluxed for 12 h. The reaction mixture was cooled to room temperature and filtered, the residue was washed with water three times, then washed with methanol two times and dried under infrared lamp to get corresponding product **3**.

6.4. Spectroscopy data of compounds **3a**–**3g**

6.4.1. 6-Cinnamoyl-2H-benzo[b][1,4]oxazin-3(4H)-one (**3a**)

Yield 55.2%, yellow solid, mp 245–247 °C. IR (KBr), ν/cm^{-1}: 3456 (NH), 1692 (C=O), 1651 (C=O). ^{1}H NMR (DMSO, 400 MHz): $\delta = 10.87$ (s, 1H, NH), 7.91 (dd, $J_1 = 2.04$, $J_2 = 8.36$ Hz, 1H, CH), 7.46–7.89 (m, 8H, ArH), 7.10 (d, $J = 8.36$ Hz, 1H, CH), 4.72 (s, 2H, CH_2). ^{13}C NMR (DMSO, 100 MHz): $\delta = 187.82$, 164.63, 147.89, 144.04, 135.17, 132.45, 131.03, 129.40 (2C), 129.26 (2C), 128.01, 125.42, 122.29, 116.43, 116.13, 67.25. HRMS calcd for $C_{17}H_{14}NO_3$ $[M+H]^+$: 280.0974, found: 280.0973.

6.4.2. 6-(3-(Benzo[d][1,3]dioxol-5-yl)acryloyl)-2H-benzo[b][1,4]oxazin-3(4H)-one(**3b**)

Yield 45.2%, yellow solid, mp 267–268 °C. IR (KBr), ν/cm^{-1}: 3444 (NH), 1693 (C=O), 1651 (C=O) cm^{-1}. ^{1}H NMR (DMSO, 300 MHz): $\delta = 10.86$ (s, 1H, NH), 7.91 (dd, $J_1 = 2.1$, $J_2 = 8.4$ Hz, 1H, CH), 6.98–7.77 (m, 6H, ArH), 7.08 (d, $J = 8.4$ Hz, 1H, CH), 6.11 (s, 2H, CH_2), 4.70 (s, 2H, CH_2). ^{13}C NMR (DMSO, 75 MHz): $\delta = 187.14$, 164.13, 149.48, 148.07, 147.24, 143.55, 132.20, 129.21, 127.46, 125.72, 124.80, 119.77, 115.83, 115.58, 108.50, 106.88, 101.62, 66.75. HRMS calcd for $C_{18}H_{14}NO_5$ $[M+H]^+$: 324.0872, found: 324.0859.

6.4.3. 6-(3-(3,5-Dimethoxyphenyl)acryloyl)-2H-benzo[b][1,4]oxazin-3(4H)-one (**3c**)

Yield 63.8%, light yellow solid, mp 240–241 °C. IR (KBr), ν/cm^{-1}: 3443 (NH), 1697 (C=O), 1656 (C=O). ^{1}H NMR (DMSO, 400 MHz): $\delta = 10.88$ (s, 1H, NH), 7.93 (dd, $J_1 = 2.04$, $J_2 = 8.44$ Hz, 1H, CH), 6.59–7.52 (m, 6H, ArH), 7.10 (d, $J = 8.40$ Hz, 1H, CH), 4.72 (s, 2H, CH_2), 3.81 (s, 6H, CH_3). ^{13}C NMR (DMSO, 75 MHz): $\delta = 187.51$, 164.24, 160.85 (2C), 147.56, 143.78, 136.76, 132.08, 127.66, 125.14, 122.46, 116.01, 115.80, 106.78 (2C), 102.91, 66.90, 55.56 (2C). HRMS calcd for $C_{19}H_{18}NO_5$ $[M+H]^+$: 340.1185, found: 340.1180.

6.4.4. 6-(3-(2,4-Dimethoxyphenyl)acryloyl)-2H-benzo[b][1,4]oxazin-3(4H)-one (**3d**)

Yield 53.4%, yellow solid, mp 222–223 °C. IR (KBr), ν/cm^{-1}: 3449 (NH), 1697 (C=O), 1642 (C=O). ^{1}H NMR (DMSO, 300 MHz): $\delta = 10.85$ (s, 1H, NH), 7.79 (dd, $J_1 = 1.8$, $J_2 = 8.4$ Hz, 1H, CH), 6.61–7.96 (m, 6H, ArH), 7.09 (d, $J = 8.4$ Hz, 1H, CH), 4.70 (s, 2H, CH_2), 3.91 (s, 3H, CH_3), 3.85 (s, 3H, CH_3). ^{13}C NMR (DMSO, 75 MHz): $\delta = 187.28$, 164.15, 163.00, 159.96, 147.04, 138.50, 132.44, 130.33, 127.38, 124.38, 118.86, 115.93, 115.57, 106.31, 98.34, 66.75, 55.81, 55.51. HRMS calcd for $C_{19}H_{18}NO_5$ $[M+H]^+$: 340.1185, found: 340.1172.

6.4.5. 6-(3-(4-(Benzyloxy)phenyl)acryloyl)-2H-benzo[b][1,4]oxazin-3(4H)-one (**3e**)

Yield 53.8%, yellow solid, mp 258–259 °C. IR (KBr), ν/cm^{-1}: 3445 (NH), 1704 (C=O), 1646 (C=O). ^{1}H NMR (DMSO, 400 MHz): $\delta = 10.86$ (s, 1H, NH), 7.79 (dd, $J_1 = 1.96$, $J_2 = 8.44$ Hz, 1H, CH), 7.07–7.84 (m, 6H, ArH), 7.09 (d, $J = 8.4$ Hz, 1H, CH), 5.19 (s, 2H, CH_2), 4.70 (s, 2H, CH_2). ^{13}C NMR (DMSO, 75 MHz): $\delta = 187.19$, 164.14, 160.36, 147.20, 143.44, 136.68, 132.25, 130.62 (2C), 128.43 (2C), 127.91, 127.73 (2C), 127.52, 127.49, 124.66, 119.41, 115.86, 115.62, 115.3 (2C), 69.38, 66.75. HRMS calcd for $C_{24}H_{20}NO_4$ $[M+H]^+$: 386.1392, found: 386.1366.

6.4.6. 6-(3-(4-Chlorophenyl)acryloyl)-2H-benzo[b][1,4]oxazin-3(4H)-one (**3f**)

Yield 63%, light yellow solid, mp 297–298 °C. IR (KBr), ν/cm^{-1}: 3463 (NH), 1706 (C=O), 1651 (C=O). ^{1}H NMR (DMSO, 400 MHz): $\delta = 10.88$ (s, 1H, NH), 7.92 (d, $J = 8.5$ Hz, 1H, CH), 7.52–7.92 (m, 7H, ArH), 7.10 (d, $J = 8.40$ Hz, 1H, CH), 4.72 (s, 2H, CH_2). HRMS calcd for $C_{17}H_{13}ClNO_3$ $[M+H]^+$: 314.0584, found: 314.0540.

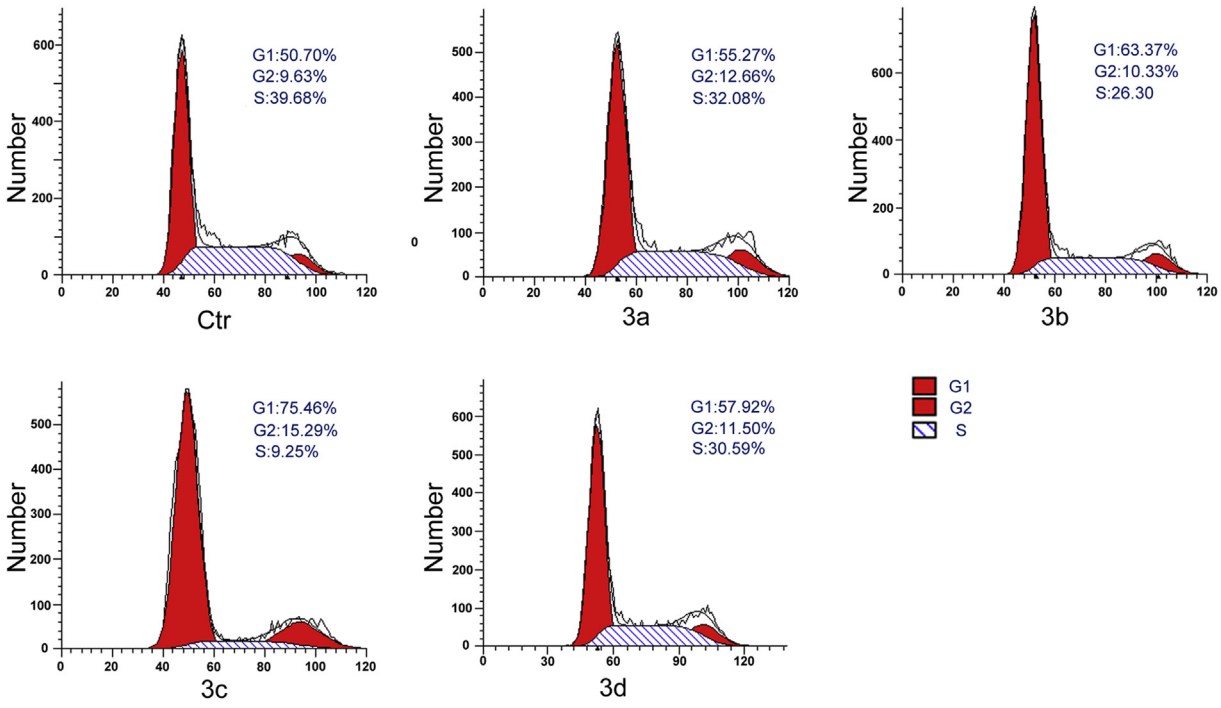

Fig. 6. Effects of compounds **3a**–**3d** (5 μM) on cell cycle distribution of A549 cells after treatment for 48 h. The values represented three independent experimental results.

*6.4.7. 6-(3-(Naphthalen-2-yl)acryloyl)-2H-benzo[b][1,4]oxazin-3(4H)-one (**3g**)*

Yield 41.3%, white solid, mp 272–274 °C (ref. 272–273 °C [14,49]). IR (KBr), ν/cm^{-1}: 3448 (NH), 1696 (C═O), 1649 (C═O). ^{1}H NMR (DMSO, 400 MHz) δ = 10.89 (s, 1H, NH), 7.60–8.55 (m, 11H, ArH, CH), 7.12 (d, J = 8.40 Hz, 1H, CH), 4.73 (s, 2H, CH_2). HRMS calcd for $C_{21}H_{16}NO_3$ $[M+H]^+$: 330.1130, found: 330.1086.

6.5. X-ray crystallography

Suitable single crystals of **3a** for X-ray structural analysis were obtained by slow evaporation of a solution of the solid in ethyl acetate at room temperature for 5 days. The crystals **3a** were mounted on a Bruker Smart Apex II CCD equipped with a graphite monochromated MoKα radiation (λ = 0.71073 Å) by using φ and ω scan modes and the data were collected at 298(2) K. The structure of the crystal was solved by direct methods and refined by full-matrix least-squares techniques implemented in the SHELXTL-97 crystallographic software.

6.6. Cell culture

Human lung cancer cell line A549 were cultured in RPMI-1640 medium at 37 °C in 5% CO_2, supplemented with 10% (v/v) bovine calf serum and 80 U/ml penicillin/streptomycin. The cells were seeded onto 24-well plates or other appropriate dishes at a number of 20,000 cells/ml.

6.7. Cell viability assay (SRB)

As previously reported, A549 cells were seeded onto 96-well plates, then treated with 0.1% DMSO (as control) or the compounds **3a**–**3g** at 1, 5 and 10 μM for 48 h, respectively. Cell viability was determined by sulforhodamine B (SRB) assay, according to the method of Skehan. Light Absorption was measured at the wavelength of 540 nm using a SpectraMAX190 microplate spectrophotometer (GMI Co, USA).

6.8. LDH assay

Cell culture medium was gathered after 48 h treatment with compounds **3a**–**3d** (10 μM) or 0.1% DMSO (as control). LDH assay was performed using a Lactate Dehydrogenase (LDH) kit (Nanjing Jiancheng Co, China), according to the manufacturer's instructions.

6.9. Acridine orange (AO) staining

After treatment with compounds **3a**–**3d** (5 μM) for 48 h, A549 cells were stained with acridine orange (5 μg/ml) for 1 min at room temperature. Then cells were washed with PBS twice and observed under an Olympus (Japan) BH-2 fluorescence microscope.

6.10. Western blot analysis

As described previously, cells were washed twice with ice cold PBS and were then lysed in protein lysis buffer (Shanghai beyotime Co., China). The protein concentration of the cells was determined by Bradford method. Following electrophoresis, the resolved protein was electrophoretically transferred to a Polyvinylidene Fluoride (PVDF) membrane (Millipore, MA, USA). The membrane was blocked with 5% non-fat milk in PBST (PBS containing 0.05% Tween 20) for 1 h at room temperature. Subsequently the membrane was probed with Rabbit anti-human LC3b antibody and anti-GAPDH mouse monoclonal antibody overnight at 4 °C, and was then washed 3 times with PBST, each time for 5 min. The membrane was subsequently incubated with HRP-conjugated goat anti-rabbit IgG or polyclonal rabbit anti-mouse immunoglobulins/HRP for 1 h at room temperature and then washed 3 times with PBST. Then the membrane was incubated with HRP substrate for 5 min and the fluorescence signals were detected with X-ray films. The relative

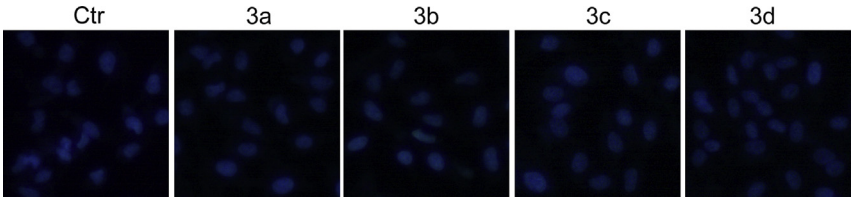

Fig. 7. Effects of compounds **3a**–**3d** (5 μM) on A549 cell apoptosis after treatment for 48 h. Microscopic photographs (200×) were taken under a fluorescent microscope (Nikon).

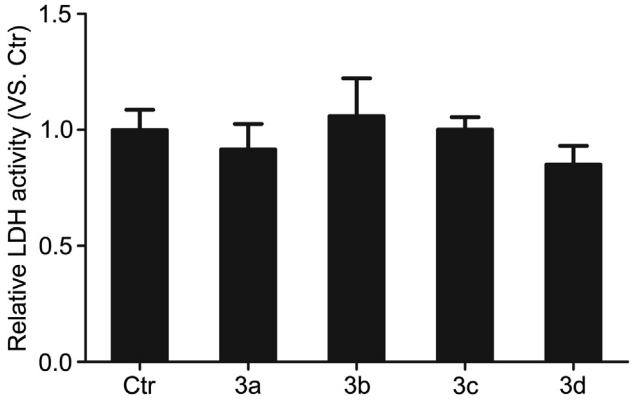

Fig. 8. Effects of compounds **3a**–**3d** on LDH release in A549 cells. Cells were treated with compounds **3a**–**3d** (10 μM) or left untreated (control) for 48 h. Results are presented as mean ± SE; $n = 3$.

quantity of proteins was analyzed by Image J software and normalized to loading controls.

6.11. Flow cytometric analysis of cell cycle distribution

Following treated with compounds **3a**–**3d** (5 μM) for 48 h, the A549 cells were harvested and fixed with 70% ethanol, then stained with 50 μg/ml propidium iodide (PI) containing 10 μg/ml RNase A at 4 °C for 1 h. The stained cells were analyzed using a FACS Calibur flow cytometer (BD Bioscience, USA). The cell cycle distribution was analyzed by ModiFit software (BD Bioscience, USA).

6.12. Hoechst 33258 staining

After treatment with 0.1% DMSO (as control) or compounds **3a**–**3d** (5 μM) for 48 h, the A549 cells in 24-well plates were stained with 10 μg/ml Hoechst 33258 for 30 min at 37 °C. Then, the cells were gently washed with PBS for twice and photographed using an Olympus (Japan) BH-2 fluorescence microscope.

6.13. Statistical analyses

Data were presented as means ± SE and analyzed by SPSS (Statistical Package for the Social Sciences) software. Pictures were processed with Adobe Photoshop software. The mean values were derived from at least 3 independent experiments. Differences with a $p < 0.05$ were considered statistically significant.

Acknowledgments

This study was supported by National Natural Science Foundation of China (20972088 and 90813022).

Appendix A. Supplementary data

Supplementary data related to this article can be found at http://dx.doi.org/10.1016/j.ejmech.2014.03.087.

References

[1] J.R. Molina, P. Yang, S.D. Cassivi, S.E. Schild, A.A. Adjei, Non-small cell lung cancer: epidemiology, risk factors, treatment, and survivorship, Mayo Clinic Proceedings 83 (2008) 584–594.
[2] C. Godugu, A.R. Patel, R. Doddapaneni, S. Marepally, T. Jackson, M. Singh, Inhalation delivery of Telmisartan enhances intratumoral distribution of nanoparticles in lung cancer models, Journal of Controlled Release 172 (2013) 86–95.
[3] W.P. Hu, H.S. Yu, Y.R. Chen, Y.M. Tsai, Y.K. Chen, C.C. Liao, L.S. Chang, J.J. Wang, Synthesis and biological evaluation of thiobenzanilides as anticancer agents, Bioorganic & Medicinal Chemistry 16 (2008) 5295–5302.
[4] A.J. Alberg, M.V. Brock, J.M. Samet, Epidemiology of lung cancer: looking to the future, Journal of Clinical Oncology 23 (2005) 3175–3185.
[5] B.A. Baldo, N.H. Pham, Adverse reactions to targeted and non-targeted chemotherapeutic drugs with emphasis on hypersensitivity responses and the invasive metastatic switch, Cancer and Metastasis Reviews 32 (2013) 723–761.
[6] S. Lian, H. Su, B.X. Zhao, W.Y. Liu, L.W. Zheng, J.Y. Miao, Synthesis and discovery of pyrazole-5-carbohydrazide N-glycosides as inducer of autophagy in A549 lung cancer cells, Bioorganic & Medicinal Chemistry 17 (2009) 7085–7092.
[7] D.J. Taatjes, B.E. Sobel, R.C. Budd, Morphological and cytochemical determination of cell death by apoptosis, Histochemistry and Cell Biology 129 (2008) 33–43.
[8] M. Packiarajan, C.G. Mazza Ferreira, S.P. Hong, A.D. White, G. Chandrasena, X. Pu, R.M. Brodbeck, A.J. Robichaud, N-Aryl pyrrolidinonyl oxadiazoles as potent mGluR5 positive allosteric modulators, Bioorganic & Medicinal Chemistry Letters 22 (2012) 5658–5662.
[9] L. Wu, K. Lu, M. Packiarajan, V. Jubian, G. Chandrasena, T.C. Wolinsky, M.W. Walker, Indolyl and dihydroindolyl N-glycinamides as potent and in vivo active NPY5 antagonists, Bioorganic & Medicinal Chemistry Letters 22 (2012) 2167–2171.
[10] W.H. Wu, T.Y. Chen, R.W. Lu, S.T. Chen, C.C. Chang, Benzoxazinoids from Scoparia dulcis (sweet broomweed) with antiproliferative activity against the DU-145 human prostate cancer cell line, Phytochemistry 83 (2012) 110–115.
[11] H.M. Niemeyer, Hydroxamic acids derived from 2-hydroxy-2H-1,4-benzoxazin-3(4H)-one: key defense chemicals of cereals, Journal of Agricultural and Food Chemistry 57 (2009) 1677–1696.
[12] A. Wang, C.P. Prouty, P.D. Pelton, M. Yong, K.T. Demarest, W.V. Murray, G.H. Kuo, Synthesis and discovery of 2,3-dihydro-3,8-diphenylbenzo[1,4] oxazines as a novel class of potent cholesteryl ester transfer protein inhibitors, Bioorganic & Medicinal Chemistry Letters 20 (2010) 1432–1435.
[13] A.N. Matralis, M.G. Katselou, A. Nikitakis, A.P. Kourounakis, Novel benzoxazine and benzothiazine derivatives as multifunctional antihyperlipidemic agents, Journal of Medicinal Chemistry 54 (2011) 5583–5591.
[14] T. Hasui, N. Matsunaga, T. Ora, N. Ohyabu, N. Nishigaki, Y. Imura, Y. Igata, H. Matsui, T. Motoyaji, T. Tanaka, N. Habuka, S. Sogabe, M. Ono, C.S. Siedem, T.P. Tang, C. Gauthier, L.A. De Meese, S.A. Boyd, S. Fukumoto, Identification of benzoxazin-3-one derivatives as novel, potent, and selective nonsteroidal mineralocorticoid receptor antagonists, Journal of Medicinal Chemistry 54 (2011) 8616–8631.
[15] P.S. Filippou, E.N. Koini, T. Calogeropoulou, P. Kalliakmani, C.A. Panagiotidis, D.A. Kyriakidis, Regulation of the Escherichia coli AtoSC two component system by synthetic biologically active 5;7;8-trimethyl-1;4-benzoxazine analogues, Bioorganic & Medicinal Chemistry 19 (2011) 5061–5070.
[16] B. Geng, J. Comita-Prevoir, C.J. Eyermann, F. Reck, S. Fisher, Exploring left-hand-side substitutions in the benzoxazinone series of 4-amino-piperidine bacterial type IIa topoisomerase inhibitors, Bioorganic & Medicinal Chemistry Letters 21 (2011) 5432–5435.
[17] H.B. Borate, S.R. Maujan, S.P. Sawargave, M.A. Chandavarkar, S.R. Vaiude, V.A. Joshi, R.D. Wakharkar, R. Iyer, R.G. Kelkar, S.P. Chavan, S.S. Kunte, Fluconazole analogues containing 2H-1,4-benzothiazin-3(4H)-one or 2H-1,4-benzoxazin-3(4H)-one moieties, a novel class of anti-Candida agents, Bioorganic & Medicinal Chemistry Letters 20 (2010) 722–725.

[18] R. Fringuelli, D. Pietrella, F. Schiaffella, A. Guarraci, S. Perito, F. Bistoni, A. Vecchiarelli, Anti-Candida albicans properties of novel benzoxazine analogues, Bioorganic & Medicinal Chemistry 10 (2002) 1681–1686.
[19] R. Fringuelli, N. Giacche, L. Milanese, E. Cenci, A. Macchiarulo, A. Vecchiarelli, G. Costantino, F. Schiaffella, Bulky 1,4-benzoxazine derivatives with antifungal activity, Bioorganic & Medicinal Chemistry 17 (2009) 3838–3846.
[20] C. Rajitha, P.K. Dubey, V. Sunku, F.J. Piedrafita, V.R. Veeramaneni, M. Pal, Synthesis and pharmacological evaluations of novel 2H-benzo[b][1,4]oxazin-3(4H)-one derivatives as a new class of anti-cancer agents, European Journal of Medicinal Chemistry 46 (2011) 4887–4896.
[21] T. Honda, T. Terao, H. Aono, M. Ban, Synthesis of novel 1,4-benzoxazin-3-one derivatives as inhibitors against tyrosine kinases, Bioorganic & Medicinal Chemistry 17 (2009) 699–708.
[22] T. Hasui, T. Ohra, N. Ohyabu, K. Asano, H. Matsui, A. Mizukami, N. Habuka, S. Sogabe, S. Endo, C.S. Siedem, T.P. Tang, C. Gauthier, L.A. De Meese, S.A. Boyd, S. Fukumoto, Design, synthesis, and structure-activity relationships of dihydrofuran-2-one and dihydropyrrol-2-one derivatives as novel benzoxazin-3-one-based mineralocorticoid receptor antagonists, Bioorganic & Medicinal Chemistry 21 (2013) 5983–5994.
[23] K.T. Nguyen, F. Li, G. Poda, D. Smil, M. Vedadi, M. Schapira, Strategy to target the substrate binding site of SET domain protein methyltransferases, Journal of Chemical Information and Modeling 53 (2013) 681–691.
[24] S. Bano, K. Javed, S. Ahmad, I.G. Rathish, S. Singh, M. Chaitanya, K.M. Arunasree, M.S. Alam, Synthesis of some novel chalcones, flavanones and flavones and evaluation of their anti-inflammatory activity, European Journal of Medicinal Chemistry 65 (2013) 51–59.
[25] A. Gomez-Rivera, H. Aguilar-Mariscal, N. Romero-Ceronio, L.F. Roa-de la Fuente, C.E. Lobato-Garcia, Synthesis and anti-inflammatory activity of three nitro chalcones, Bioorganic & Medicinal Chemistry Letters 23 (2013) 5519–5522.
[26] N.A. Shakil, M.K. Singh, M. Sathiyendiran, J. Kumar, J.C. Padaria, Microwave synthesis, characterization and bio-efficacy evaluation of novel chalcone based 6-carbethoxy-2-cyclohexen-1-one and 2H-indazol-3-ol derivatives, European Journal of Medicinal Chemistry 59 (2013) 120–131.
[27] V. Sharma, G. Singh, H. Kaur, A.K. Saxena, M.P. Ishar, Synthesis of beta-ionone derived chalcones as potent antimicrobial agents, Bioorganic & Medicinal Chemistry Letters 22 (2012) 6343–6346.
[28] K. Liaras, A. Geronikaki, J. Glamoclija, A. Ciric, M. Sokovic, Novel (E)-1-(4-methyl-2-(alkylamino)thiazol-5-yl)-3-arylprop-2-en-1-ones as potent antimicrobial agents, Bioorganic & Medicinal Chemistry 19 (2011) 7349–7356.
[29] X. Jin, C.J. Zheng, M.X. Song, Y. Wu, L.P. Sun, Y.J. Li, L.J. Yu, H.R. Piao, Synthesis and antimicrobial evaluation of L-phenylalanine-derived C5-substituted rhodanine and chalcone derivatives containing thiobarbituric acid or 2-thioxo-4-thiazolidinone, European Journal of Medicinal Chemistry 56 (2012) 203–209.
[30] M. Goodarzi, W. Saeys, M.C. de Araujo, R.K. Galvao, Y. Vander Heyden, Binary classification of chalcone derivatives with LDA or KNN based on their antileishmanial activity and molecular descriptors selected using the successive projections algorithm feature-selection technique, European Journal of Pharmaceutical Sciences 51 (2014) 189–195.
[31] M. Roussaki, B. Hall, S.C. Lima, A.C. da Silva, S. Wilkinson, A. Detsi, Synthesis and anti-parasitic activity of a novel quinolinone-chalcone series, Bioorganic & Medicinal Chemistry Letters 23 (2013) 6436–6441.
[32] A.V. Saranya, S. Ravi, In-vitro acetylcholine esterase inhibition activity of chalcones with phenothiazine moiety, Research Journal of Recent Sciences 12 (2012) 40–43.
[33] K.V. Sashidhara, G.R. Palnati, R. Sonkar, S.R. Avula, C. Awasthi, G. Bhatia, Coumarin chalcone fibrates: a new structural class of lipid lowering agents, European Journal of Medicinal Chemistry 64 (2013) 422–431.
[34] T.A. Dias, C.L. Duarte, C.F. Lima, M.F. Proenca, C. Pereira-Wilson, Superior anticancer activity of halogenated chalcones and flavonols over the natural flavonol quercetin, European Journal of Medicinal Chemistry 65 (2013) 500–510.
[35] H. Wei, X. Zhang, G. Wu, X. Yang, S. Pan, Y. Wang, J. Ruan, Chalcone derivatives from the fern Cyclosorus parasiticus and their anti-proliferative activity, Food and Chemical Toxicology 60 (2013) 147–152.
[36] R. Abonia, D. Insuasty, J. Castillo, B. Insuasty, J. Quiroga, M. Nogueras, J. Cobo, Synthesis of novel quinoline-2-one based chalcones of potential anti-tumor activity, European Journal of Medicinal Chemistry 57 (2012) 29–40.
[37] M. Abdel-Aziz, S.E. Park, D. Abuo-Rahma Gel, M.A. Sayed, Y. Kwon, Novel N-4-piperazinyl-ciprofloxacin-chalcone hybrids: synthesis, physicochemical properties, anticancer and topoisomerase I and II inhibitory activity, European Journal of Medicinal Chemistry 69 (2013) 427–438.
[38] S.Y. Kim, I.S. Lee, A. Moon, 2-Hydroxychalcone and xanthohumol inhibit invasion of triple negative breast cancer cells, Chemico-Biological Interactions 203 (2013) 565–572.
[39] S.W. Ryter, A.M. Choi, Autophagy in the lung, Proceedings of the American Thoracic Society 7 (2010) 13–21.
[40] D.S. Arroyo, E.A. Gaviglio, J.M. Peralta Ramos, C. Bussi, M.C. Rodriguez-Galan, P. Iribarren, Autophagy in inflammation, infection, neurodegeneration and cancer, International Immunopharmacology 18 (2013) 55–65.
[41] F. Janku, D.J. McConkey, D.S. Hong, R. Kurzrock, Autophagy as a target for anticancer therapy, Nature Reviews. Clinical Oncology 8 (2011) 528–539.
[42] D.C. Rubinsztein, P. Codogno, B. Levine, Autophagy modulation as a potential therapeutic target for diverse diseases, Nature Reviews. Drug Discovery 11 (2012) 709–730.
[43] P. Bischoff, E. Josset, F.J. Dumont, Novel pharmacological modulators of autophagy and therapeutic prospects, Expert Opinion on Therapeutic Patents 22 (2012) 1053–1079.
[44] M. Mahmoudi, K. Azadmanesh, M.A. Shokrgozar, W.S. Journeay, S. Laurent, Effect of nanoparticles on the cell life cycle, Chemical Reviews 111 (2011) 3407–3432.
[45] X.S. Ren, M.H. Yin, X. Zhang, Z. Wang, S.P. Feng, G.X. Wang, Y.J. Luo, P.Z. Liang, X.Q. Yang, J.X. He, B.L. Zhang, Tumor-suppressive microRNA-449a induces growth arrest and senescence by targeting E2F3 in human lung cancer cells, Cancer Letters 344 (2014) 195–203.
[46] B.R. You, H.R. Shin, W.H. Park, PX-12 inhibits the growth of A549 lung cancer cells via G2/M phase arrest and ROS-dependent apoptosis, International Journal of Oncology 44 (2014) 301–308.
[47] I.R. Indran, G. Tufo, S. Pervaiz, C. Brenner, Recent advances in apoptosis, mitochondria and drug resistance in cancer cells, Biochimica et Biophysica Acta 1807 (2011) 735–745.
[48] L.A. Booth, S. Tavallai, H.A. Hamed, N. Cruickshanks, P. Dent, The role of cell signalling in the crosstalk between autophagy and apoptosis, Cellular Signalling 26 (2013) 549–555.
[49] T. Moreira Osorio, F. Delle Monache, L. Domeneghini Chiaradia, A. Mascarello, T. Regina Stumpf, C. Roberto Zanetti, D. Bardini Silveira, C. Regina Monte Barardi, E. de Fatima Albino Smania, A. Viancelli, L. Ariel Totaro Garcia, R. Augusto Yunes, R. Jose Nunes, A. Smania Jr., Antibacterial activity of chalcones, hydrazones and oxadiazoles against methicillin-resistant Staphylococcus aureus, Bioorganic & Medicinal Chemistry Letters 22 (2012) 225–230.